Forkhead box N4 (Foxn4) activates Dll4-Notch signaling to suppress photoreceptor cell fates of early retinal progenitors

Huijun Luo[a,1], Kangxin Jin[a], Zhenhui Xie[a], Feng Qiu[a], Shengguo Li[a], Min Zou[a], Li Cai[b], Katsuto Hozumi[c], David T. Shima[d], and Mengqing Xiang[a,2]

[a]Center for Advanced Biotechnology and Medicine and Department of Pediatrics, University of Medicine and Dentistry of New Jersey–Robert Wood Johnson Medical School, Piscataway, NJ 08854; [b]Department of Biomedical Engineering, Rutgers University, Piscataway, NJ 08854; [c]Department of Immunology and Research Center for Embryogenesis and Organogenesis, Tokai University School of Medicine, Kanagawa 259-1193, Japan; and [d]Laboratory for Translational Vision Research, University College London Institute of Ophthalmology, London EC1V 9EL, United Kingdom

The generation of diverse neuronal types and subtypes from multipotent progenitors during development is crucial for assembling functional neural circuits in the adult central nervous system. During mouse retinogenesis, early retinal progenitors give rise to several cell types, including ganglion, amacrine, horizontal, cone, and rod cells. It is unknown at present how each of these fates is selected from the multiple neuronal fates available to the early progenitor. By using a combination of bioinformatic, genetic, and biochemical approaches, we investigated the mechanism by which Foxn4 selects the amacrine and horizontal cell fates from multipotential retinal progenitors. These studies indicate that Foxn4 has an intrinsic activity to suppress the alternative photoreceptor cell fates of early retinal progenitors by selectively activating Dll4-Notch signaling. Gene expression and conditional ablation analyses reveal that *Dll4* is directly activated by Foxn4 via phylogenetically conserved enhancers and that Dll4 can partly mediate the Foxn4 function by serving as a major Notch ligand to expand the progenitor pool and limit photoreceptor production. Our data together define a Foxn4-mediated molecular and signaling pathway that underlies the suppression of alternative cell fates of early retinal progenitors.

forkhead/winged-helix transcription factor | proneural bHLH gene | Crx | Otx2

During vertebrate development, neurons are usually specified and differentiated from multipotent progenitor cells that are capable of producing two or more types of neurons and glial cells. For instance, during mouse retinogenesis, embryonic retinal progenitors are able to generate several early-born cell types including ganglion, amacrine, horizontal, cone, and rod cells; and postnatal progenitors can generate several late-born cell types including rod, bipolar, and Müller glial cells (1, 2). Production of these diverse retinal cell types is essential for assembling a functional retinal circuitry consisting of rods and cones as photoreceptors; amacrine, horizontal, and bipolar cells as interneurons; and retinal ganglion cells (RGCs) as output neurons. It has been proposed that intrinsic and extrinsic factors together determine the choice of retinal cell fates and that the progenitors may pass through successive and distinct states of competence for the ordered generation of different cell types (3–5). At present, however, there is little known about the molecular basis of competence states and how a particular cell fate is selected from the multiple fates available to a retinal progenitor.

During retinogenesis, neuroepithelial cells in the optic vesicle must acquire multipotency and establish competence for the generation of the full range of retinal cell types. Genetic ablation studies have demonstrated that the Pax6 and Sox2 transcription factors (TFs) are required to coordinately confer multipotency to retinal progenitors (6–8), and that the Ikzf1/Ikaros zinc finger TF plays a key role in establishing the early temporal competence

stages responsible for generating early-born cell types (9). We have shown previously that the forkhead/winged helix TF Foxn4 is required by early retinal progenitors to establish the competence for the generation of amacrine and horizontal cells. Loss of Foxn4 function eliminates most amacrine cells and all horizontal cells and causes a progenitor fate switch to photoreceptors (10). Foxn4 appears to regulate progenitor competence in part by activating the expression of proneural bHLH TF genes *Ptf1a*, *Neurod1*, and *Neurod4/Math3* (10), which are required for the specification of amacrine and/or horizontal cells (11–13).

It has long been recognized that retinogenic TFs often play dual roles to promote certain cell fate(s) as well as suppress other fates available to a progenitor. For instance, Otx2 is required for photoreceptor generation while suppressing the amacrine cell fate (14), and Nr2e3 in association with Crx promotes the rod fate while inhibiting cone differentiation (15–17). Similarly, Atoh7 and Pou4f2 are essential for specifying RGCs while suppressing the cone, amacrine, and horizontal fates (18–20). Foxn4 appears also to confer early retinal progenitors with amacrine and horizontal competence not only by activating TF genes involved in their specification and differentiation but also by limiting the alternative fates of early progenitors. The increased photoreceptor production and *Crx* up-regulation in *Foxn4*-null retinas suggest that Foxn4 normally represses *Crx* expression, which in turn suppresses photoreceptor differentiation (10). How Foxn4 represses the expression of photoreceptor TFs is unknown—it can be direct or indirect, such as through activating Notch signaling, which has been shown to inhibit photoreceptor fates (21, 22).

In this study, we set out to explore the Foxn4-mediated molecular pathways and signaling events that lead to the suppression of the alternative photoreceptor fates of early retinal progenitors. Microarray profiling and misexpression analyses demonstrated that Foxn4 selectively activates *Dll4* expression among various Notch ligand and receptor genes. It colocalizes with Dll4 in a subset of retinal progenitors and directly activates its gene expression through phylogenetically conserved enhancers. Similar to *Foxn4* deletion, inactivating *Dll4* in retinal progenitors resulted in photoreceptor overproduction and reduced progenitor proliferation.

These data together thus suggest that Foxn4 limits alternative cell fates of early retinal progenitors in part by directly activating Dll4-Notch signaling to suppress photoreceptor production.

Results

Down-Regulation of Notch Signaling Genes in *Foxn4*-Null Mutant Retinas. To understand at the molecular level how Foxn4 may regulate the competence of embryonic retinal progenitors and bias them toward amacrine and horizontal cell fates, we carried out microarray analysis by using the Affymetrix Mouse Genome 430A arrays. Array hybridization was carried out in quadruplicates by using probes derived from embryonic day (E) 14.5 retinas of $Foxn4^{+/+}$ and $Foxn4^{lacZ/lacZ}$ embryos (10). The obtained data were analyzed by using the Affymetrix Microarray Suite and dChip software (23) to calculate fold changes of transcripts between the control and mutant. We found that 176 transcripts displayed a decrease or increase of 1.7-fold or higher in their expression levels in *Foxn4* mutant retinas. A total of 134 of them are down-regulated and 42 are up-regulated (Fig. 1 *A* and *B*; and Dataset S1). The differentially expressed genes were functionally classified according to Gene Ontology terminology by using the Database for Annotation, Visualization and Integrated Discovery, a Web-based tool (24). Among the down-regulated genes, those involved in neuron differentiation, cell fate commitment, retinal morphogenesis, and transcription are all enriched (Dataset S2), consistent with the crucial regulatory function of Foxn4 in retinal development. Notably, *Ptf1a*, *Neurod1*, *Neurod4*, and *Prox1*, which are TF genes involved in the specification of amacrine and horizontal cells (11–13, 25, 26), are down-regulated in their expression in the null retina (Fig. 1*C*). In

addition, we noted that several genes in the Notch signaling pathway are also down-regulated in the mutant (Fig. 1*C*).

Regulation of *Dll4* Notch Ligand Gene Expression by Foxn4. We carried out RNA in situ hybridization analysis for a number of Notch signaling component genes in *Foxn4* mutant retinas to verify diminished Notch signaling revealed by microarray profiling (Fig. 1). The *Dll4* ligand and *Hes5* effector genes were expressed within the outer neuroblastic layer of E14.5 WT retinas, but their expression was dramatically reduced in $Foxn4^{lacZ/lacZ}$ retinas (Fig. 2 *C*, *D*, *G*, and *H*), in agreement with the microarray data (Fig. 1*C*). Similarly, the expression of the Notch signaling integrator gene *Rbpj* was moderately decreased (Fig. S1 *A* and *B*). However, there was barely any change in the expression of *Dll1*, *Notch1*, *Hes1*, and *Hey1* genes in the null retina (Fig. 2 *A*, *B*, *E*, and *F* and Fig. S1 *C*, *D*, *G*, and *H*). The same was true for the expression of the neurogenic gene *Hes6* (Fig. S1 *E* and *F*).

Our microarray and RNA in situ hybridization analyses suggested that Foxn4 may selectively modulate *Dll4* expression among all Notch ligand genes. We investigated this possibility by determining whether misexpressed Foxn4 had the activity to induce expression of various Notch ligand and receptor genes in cultured retinal explants. Foxn4 was ectopically expressed in E17.5 retinal explants by electroporation by using the modified pCIG expression vector (Fig. 2*I*) (27), and RNA levels were measured by semiquantitative RT-PCR. We found that misexpressed Foxn4 led to a significant increase of *Dll4* transcripts in a concentration-dependent manner (Fig. 2*J*). However, it had little or no effect on the expression levels of *Dll1*, *Dll3*, *Jag1*, *Jag2*, and *Notch1-4* (Fig. 2*J*). Thus, Foxn4 is sufficient to induce ex-
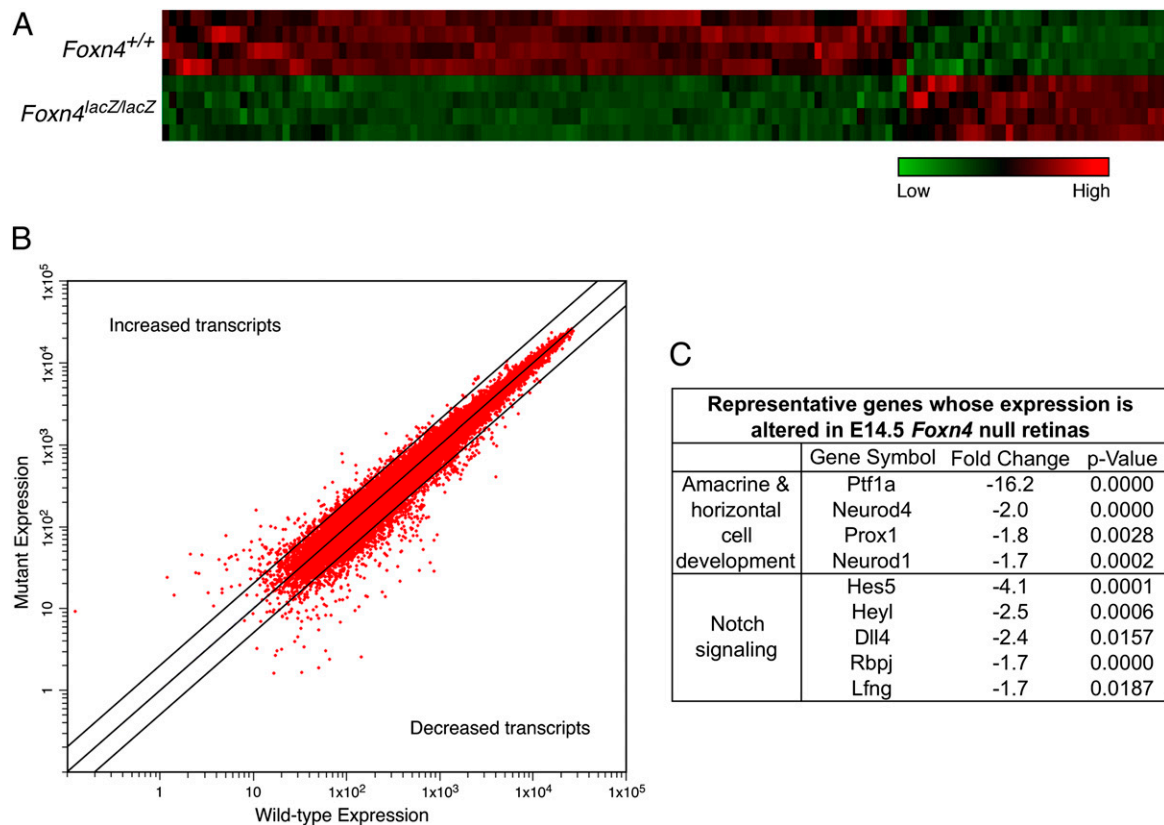
Fig. 1. Expression array analysis of genes whose expression changes in E14.5 *Foxn4^{lacZ/lacZ}* retinas. (*A*) Cluster analysis reveals a large group of down-regulated genes and a smaller group of up-regulated genes in the mutant retina. (*B*) Scatter plot of probe hybridization signals. The central diagonal line represents equal expression in the two genotypes, and the two parallel lines indicate a twofold change in expression. (*C*) Some representative genes whose expression are significantly altered in the mutant retina and which are involved in amacrine and horizontal cell development or Notch signaling.

Figure 1C table:

Representative genes whose expression is altered in E14.5 *Foxn4* null retinas

	Gene Symbol	Fold Change	p-Value
Amacrine & horizontal cell development	Ptf1a	-16.2	0.0000
	Neurod4	-2.0	0.0000
	Prox1	-1.8	0.0028
	Neurod1	-1.7	0.0002
Notch signaling	Hes5	-4.1	0.0001
	Heyl	-2.5	0.0006
	Dll4	-2.4	0.0157
	Rbpj	-1.7	0.0000
	Lfng	-1.7	0.0187

www.manaraa.com

Fig. 2. Regulation of *Dll4* expression by Foxn4. (*A–H*) RNA in situ hybridization indicated that the expression of *Dll4* and *Hes5* was greatly down-regulated in E14.5 *Foxn4^lacZ/lacZ* retinas. (*I*) Schematics of the pCIG and pCIG-Foxn4 expression plasmids. (*J*) Induction of *Dll4* expression by Foxn4. E17.5 retinal explants were transfected by electroporation with pCIG (1.0 μg/μL for lane 1) or pCIG-Foxn4 at different concentrations (0.5 μg/μL, 1.0 μg/μL, and 2.0 μg/μL for lanes 2–4, respectively). Five days after transfection, cultured retinas were collected and RNA was extracted. Semiquantitative RT-PCR was perform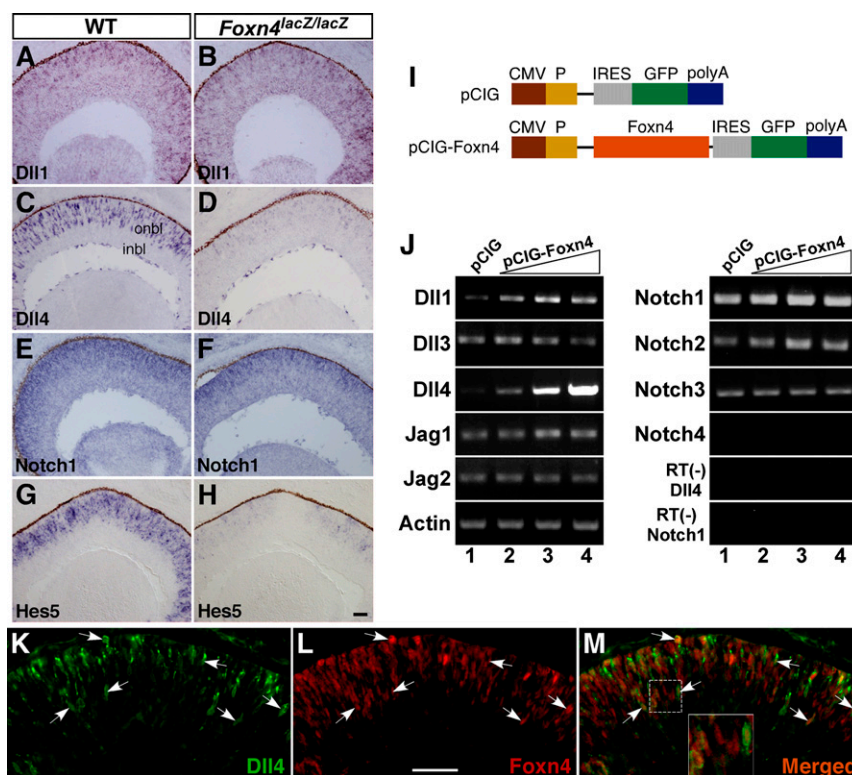ed by using gene-specific primers. β-Actin was used as an internal control to confirm that equal amount of cDNA was used in each experiment. RT-PCR was also performed in the absence of reverse transcriptase (RT) to serve as negative controls. (*K–M*) E12.5 retinal sections were double-immunostained with anti-Dll4 (green) and anti-Foxn4 (red) antibodies. The majority of Dll4-expressing cells are also immunoreactive for Foxn4. Arrows point to representative colocalized cells. (*M*) *Inset*: Outlined region at higher magnification. (Scale bars: 50 μm.)

pression of *Dll4* but not other Notch ligand or receptor genes in the developing retina. Consistent with this notion, we found by double immunofluorescence that, in E12.5 retinas, nearly all Dll4-expressing progenitor cells coexpressed Foxn4, although Foxn4 was expressed in more progenitors (Fig. 2 *K–M*). These data suggest that Foxn4 may control *Dll4* expression in the same progenitors by a cell-autonomous mechanism.

Activation of *Dll4* Expression by Foxn4 via Phylogenetically Conserved Enhancers. To assess whether Foxn4 directly activates *Dll4* expression in retinal progenitors, we took a bioinformatic approach to identify conserved noncoding sequences in the *Dll4* loci as candidate Foxn4 *cis*-regulatory elements. We used the Non-Coding Sequence Retrieval System (28) to download *Dll4* noncoding sequences from all available vertebrate species and then applied the VISTA program (29) to identify several conserved regions (CRs) in the 5′-flanking, intron, and 3′-flanking sequences (Fig. 3*A*). To test if Foxn4 activates *Dll4* expression through any of these CRs, we subcloned the conserved mouse CR1–CR4 sequences into the pBGP-DsRed reporter plasmid, which contains a minimal β-globin promoter preceding the DsRed reporter gene (Fig. 3*A* and Fig. S2*A*). The CR1 reporter construct was coelectroporated with pCIG-Foxn4 or control pCIG expression plasmids into E17.5 retinal explants, and reporter gene expression was analyzed in whole-mount retinal explants after 3 d in culture. A small number of cells were found to express DsRed in the presence of pCIG (Fig. S2 *B–D*), reflecting activation of the 5′ enhancer CR1 by endogenous transactivators. In the presence of pCIG-Foxn4, however, there

was a steep increase of DsRed-expressing cells that coexpressed Foxn4 (as visualized by GFP expression; Fig. S2 *E–G*). Similarly, Foxn4 was able to activate DsRed expression through the intronic CR3, albeit at a slightly lower level than through CR1 (Fig. S2 *A* and *I*). Thus, *Dll4* expression can be activated by Foxn4 via both the 5′ and intronic enhancers. In contrast, Foxn4 failed to activate DsRed expression through the CR2 and CR4 CRs (Fig. S2 *H* and *J*).

CR1 is a 937-bp sequence located between −4,191 bp and −3,255 bp in the *Dll4* 5′-flanking region (Fig. 3*B*). To further narrow the region that can be activated by Foxn4, we constructed a number of truncated promoter plasmids CR1a-CR1g as shown in Fig. 3*B*. When cotransfected with pCIG-Foxn4 by electroporation in retinal explants, CR1c and CR1d exhibited a similar level of DsRed expression as the full-length CR1 (Fig. 3 *B*, *C*, *F*, *G*, and *L–N*), and CR1e had greatly reduced activity (Fig. 3 *B* and *H*). However, CR1a, CR1b, CR1f, and CR1g displayed little or no DsRed reporter expression (Fig. 3 *B*, *D*, *E*, *I*, *J*, and *K*). These results thus define a critical 85-bp sequence between CR1d and CR1g that can be activated by Foxn4. It has been shown that Foxn1 binds to an 11-bp consensus sequence containing the invariant tetranucleotide 5′-ACGC, and zebrafish Foxn4 binds to 5′-TTTTACGCTTT also containing the invariant motif (30, 31). We searched for these motifs in the 85-bp sequence and found four ACGC motifs in a cluster (Fig. 3*B* and Fig. S2*K*), which may be potential Foxn4 binding sites. All four motifs are conserved in human *Dll4* and two of them are conserved in the chicken sequence (Fig. S2*K*).
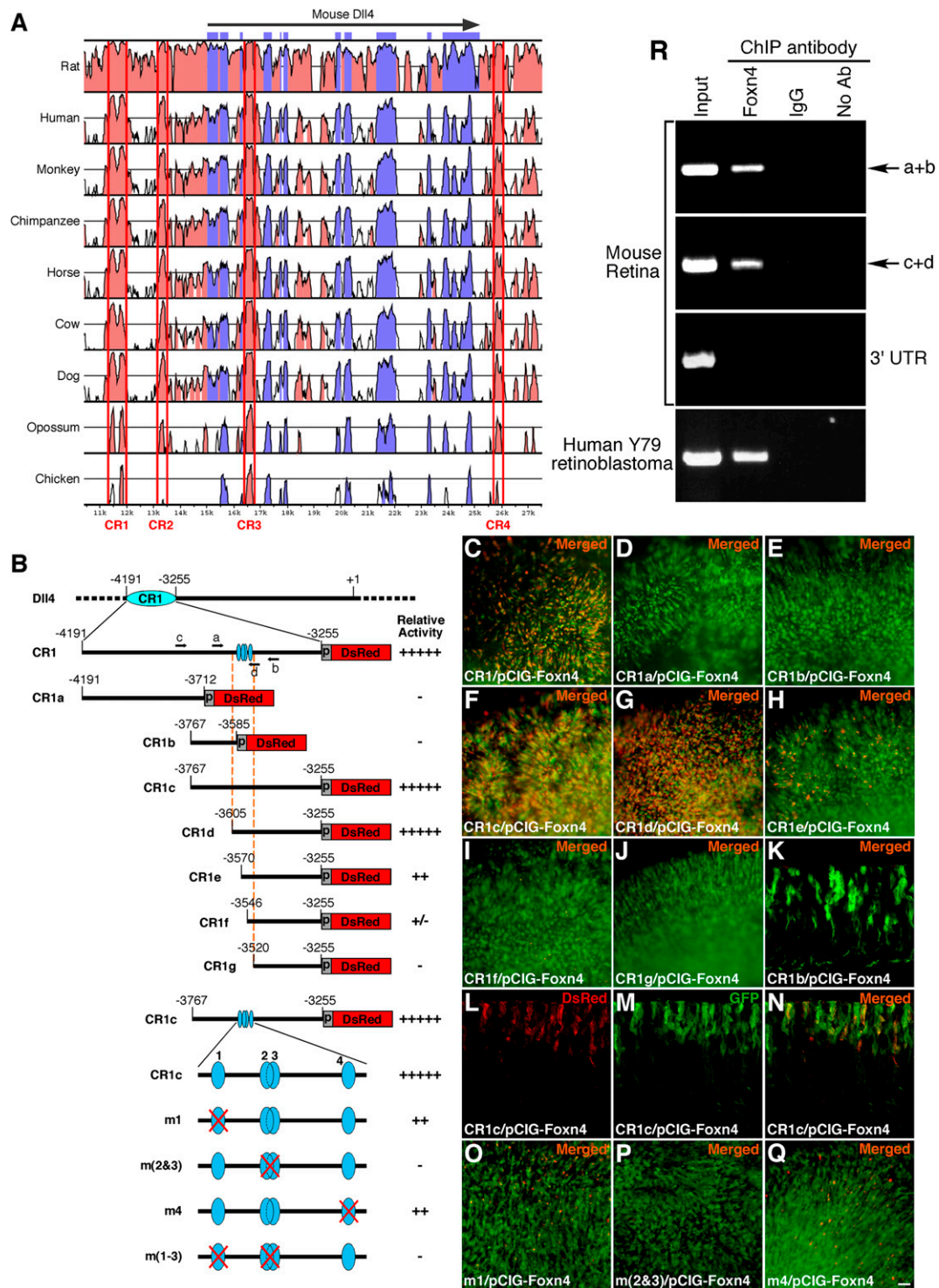
Fig. 3. Direct activation of *Dll4* expression by Foxn4 through phylogenetically conserved enhancers. (*A*) VISTA analysis identifies CRs between mouse and other vertebrate *Dll4* loci. Exons are shown in blue and conserved noncoding sequences in pink. (*B*) Schematics of truncated (CR1a-CR1g) and mutated [m1, m(2&3), m4, and m(1–3)] CR1 DsRed reporter constructs. Corresponding relative activities are indicated to the right. The four cyan ovals in the CR1 fragment indicate the clustered ACGC motifs. The vertical dashed lines outline the critical 85-bp region containing the ACGC cluster. The positions of the four primers (*a–d*) used in ChIP assay (*R*) are also indicated. (*C–Q*) DsRed expression in retinal explants coelectroporated with various CR1 reporter constructs and Foxn4 expression plasmid. Shown are images from flat-mounted explants (*C–J* and *O–Q*) or explant sections (*K–N*). As visualized in whole-mount explants, CR1c and CR1d exhibited similar high levels of DsRed expression as full-length CR1 (*C*, *F*, and *G*), whereas CR1e displayed a dramatic decrease in activity and CR1a, CR1b, CR1f, and CR1g had little or no activity (*D*, *E*, and *H–J*). In cross sections, DsRed and GFP were seen to colocalize in the same cells in retinas cotransfected with the CR1c reporter and Foxn4 expression constructs (*L–N*); however, DsRed was absent from those cotransfected with the CR1b reporter and Foxn4 expression constructs (*K*). Compared with the CR1c reporter (*F*), the mutant reporter constructs m1, m(2&3), and m4 showed greatly reduced or no DsRed expression (*O–Q*). (*R*) ChIP assay shows Foxn4 binding to a region containing the ACGC cluster but not to a 3′UTR. Chromatin DNA was prepared from mouse embryonic retinas or the Y79 human retinoblastoma cells. Input lane represents 10% of chromatin DNA used for ChIP assay. (Scale bars: *K–N*, 11.2 μm; *C–J* and *O–Q*, 50 μm.)

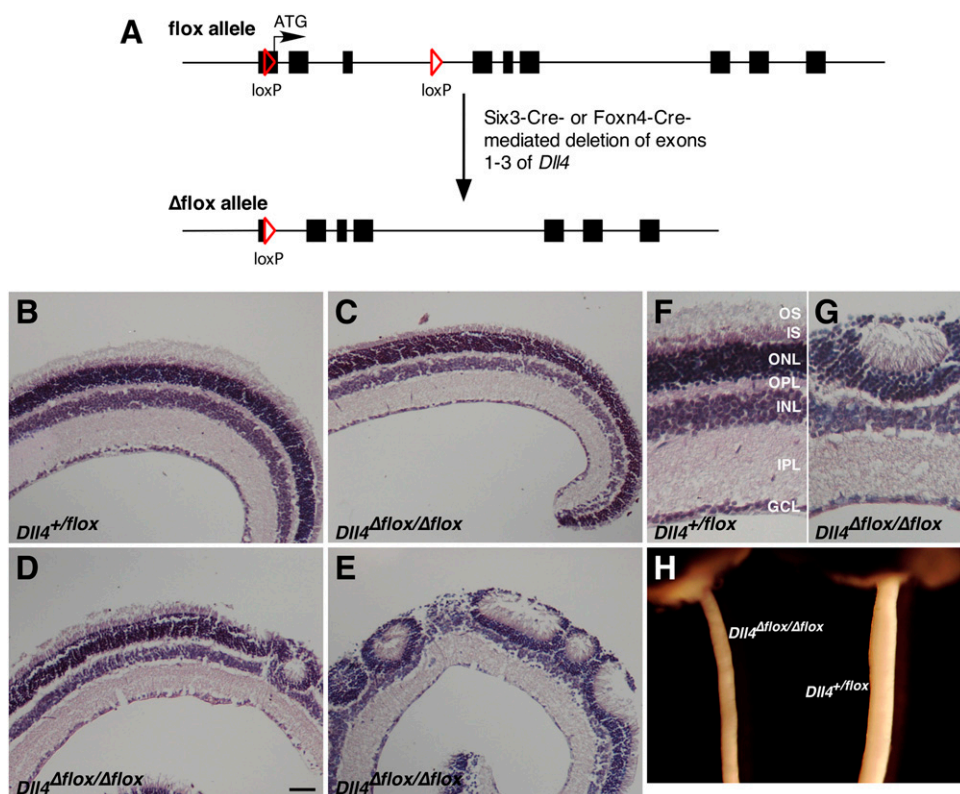**Fig. 4.** Gross abnormalities of the $Dll4^{\Delta flox/\Delta flox}$ retina. (A) A floxed $Dll4$ mouse line was bred with the Six3-Cre or Foxn4-Cre transgenic lines to delete exons 1–3 of $Dll4$ in the developing retina. (B–G) Laminar structures were visualized in P27 retinal sections by H&E staining. Compared with the control, $Dll4^{\Delta flox/\Delta flox}$ retinas are thinner in all layers. Most regions in the mutant retina are free of rosette-like structures (C). Rosettes are present only in occasional regions within the outer layers of the mutant retina (D and G), and they are rarely found in cluster (E). (H) Optic nerve diameter is greatly reduced in P21 $Dll4^{\Delta flox/\Delta flox}$ mice compared with $Dll4^{+/flox}$ littermates. GCL, ganglion cell layer; INL, inner nuclear layer; IPL, inner plexiform layer; IS, inner segment; ONL, outer nuclear layer; OPL, outer plexiform layer; OS, outer segment. (Scale bars: F and G, 25 μm; B–E, 50 μm.)

We investigated whether the ACGC motifs in the 85-bp sequence are required for Foxn4 activation by site-directed mutagenesis. When a single motif was mutagenized to AAAA in the CR1c promoter plasmid, there was a precipitous decrease in the number of DsRed-expressing cells in retinal explants cotransfected with pCIG-Foxn4 (Fig. 3 B, F, O, and Q), whereas simultaneously mutating two or three motifs completely abolished DsRed expression (Fig. 3 B and P). Thus, all four ACGC motifs appear to be synergistically required to activate $Dll4$ expression by Foxn4. To ask whether Foxn4 directly binds and occupies the 85-bp region, we carried out a ChIP assay by using chromatin DNA prepared from E14.5 to E17.5 mouse embryonic retinas. Although the control IgG did not immunoprecipitate any tested DNA fragments, an anti-Foxn4 antibody specifically precipitated CR1 fragments containing the ACGC cluster but not a 3′ UTR fragment that does not contain such a motif (Fig. 3R and Fig. S3). Moreover, the antibody was able to immunoprecipitate a similar fragment harboring the ACGC cluster in chromatin DNA prepared from the Y79 human retinoblastoma cells (Fig. 3R and Fig. S3), which have previously been shown to express Notch signaling molecules (32). Therefore, both mouse and human $Dll4$ may be directly bound and activated by Foxn4.

Overproduction of Photoreceptors in $Dll4$-Deficient Retinas. As a direct target gene of Foxn4, $Dll4$ may act to partly mediate Foxn4 function in fate specification and proliferation of retinal progenitors. To test this possibility, we conditionally inactivated $Dll4$ in retinal progenitors by using the $Dll4^{flox}$ allele and Six3-Cre or Foxn4-Cre driver mouse lines (Fig. 4A) (33–35). The Foxn4-Cre line we generated previously drives Cre expression in most retinal

progenitors as tested by crossing it with the R26R-YFP reporter line (Fig. S4). Similar mutant phenotypes were produced by using Six3-Cre or Foxn4-Cre line, so, in our analysis, $Dll4^{\Delta flox/\Delta flox}$ represented Six3-Cre;$Dll4^{flox/flox}$ or Foxn4-Cre;$Dll4^{flox/flox}$, and $Dll4^{+/flox}$ or $Dll4^{flox/flox}$ were used as controls.

At postnatal day (P) 21 to 27, when retinal development is complete, H&E staining of WT and mutant retinal sections indicated that $Dll4^{\Delta flox/\Delta flox}$ retinas were significantly thinner [thickness at intermediate region, $Dll4^{\Delta flox/\Delta flox}$, 168.9 ± 9.7 μm ($n = 8$); control, 209.2 ± 12.1 μm ($n = 8$)], with occasional regions abnormally organized into rosette-like structures in the outer nuclear layer (Fig. 4 B–G). Consequently, mutant littermates had an optic nerve with a much reduced diameter (Fig. 4H). Despite the reduced retinal thickness, however, we found that the number of recoverin-immunoreactive photoreceptors was significantly increased in P1 and P6 $Dll4^{\Delta flox/\Delta flox}$ retinas, and so was rhodopsin immunoreactivity (Fig. 5 A–F, I, J, and Y). The increased photoreceptors failed to maintain until adult stages, as there were more recoverin$^+$ photoreceptors in the WT than in the mutant at P30 (Fig. 5 G and H). Other cell types all significantly decreased in $Dll4^{\Delta flox/\Delta flox}$ retinas, which included Pax6$^+$ amacrine cells and RGCs (Fig. 5 K, L, and Y), Pou4f2$^+$ or Pou4f1$^+$ RGCs (Fig. 5 M, N, and Y), GLYT1$^+$, Gad67$^+$ or calbindin$^+$ amacrine cells (Fig. 5 O–T), calbindin$^+$ horizontal cells (Fig. 5 S, T, and Y), Chx10$^+$ bipolar cells (Fig. 5 U, V, and Y), and Sox9$^+$ or glutamine synthetase (GS)$^+$ Müller cells (Fig. 5 W–Y). Quantification of immunoreactive cells revealed that the extent of cell increase or decrease correlated with $Dll4$ gene dosage, as there were intermediate changes in $Dll4^{+/\Delta flox}$ retinas (Fig. 5Y).
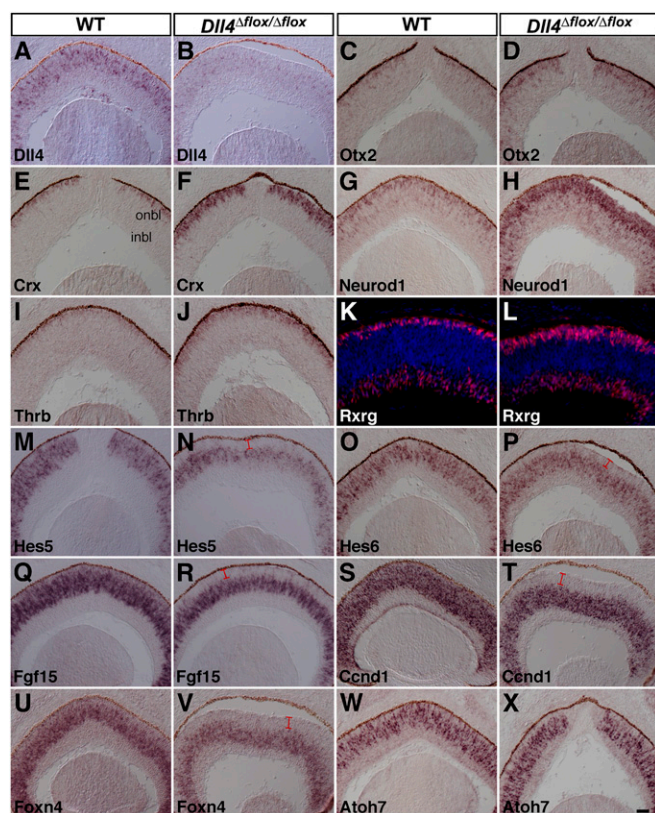
Luo et al.

Fig. 5. Altered cell generation in the $Dll4^{\Delta flox/\Delta flox}$ retina. (*A–X*) Immunofluorescent labeling of retinal sections from $Dll4^{+/flox}$ and $Dll4^{\Delta flox/\Delta flox}$ mice at the indicated stages with the indicated antibodies (red). All sections were counterstained with nuclear dyes Yopro (green) or DAPI (blue). Note the increased recoverin and rhodopsin immunoreactivity in $Dll4^{\Delta flox/\Delta flox}$ retinas at early postnatal stages despite the eventual decrease of recoverin⁺ cells at P30 (*C–J*). The immunoreactivity for other cell type-specific markers including Pax6, Pou4f2, GLYT1, Gad67, calbindin, Chx10, and Sox9 all decreased in the mutant retina (*K–X*). Arrows in *S* and *T* point to horizontal cells, and the arrowhead in *B* indicates that Dll4 expression was not ablated in the blood vessel. (*Y*) Quantification of cells that are immunoreactive for various cell type-specific markers in *Dll4* control and mutant retinas. Each histogram represents the mean ± SD for three retinas. Note that all marker-positive cells were counted in optical fields under a fluorescent microscope at a magnification of 1,000× except for calbindin⁺ horizontal cells, which were counted from entire sections, because of the paucity of this cell type. Recoverin⁺ cells were counted at P6 and all other marker-positive cells were counted at P30. GCL, ganglion cell layer; INL, inner nuclear layer; IPL, inner plexiform layer; ONL, outer nuclear layer; OPL, outer plexiform layer. (Scale bars: *I* and *J*, 12.5 μm; *A–H* and *K–X*, 36.8 μm.)

As determined by RNA in situ hybridization and immunostaining, at the outer edge of E14.5 $Dll4^{\Delta flox/\Delta flox}$ retinas, there was an increase in expression of *Otx2*, *Crx*, *Neurod1*, *Thrb/Thrb2*, and *Rxrg* (Fig. 6 *A–L*), which are all TF genes involved in cone and rod specification and differentiation (14, 17, 36–40). Thus, *Dll4* ablation leads to increased photoreceptor production, which also occurs in *Notch1* and *Foxn4* mutant retinas (10, 21, 22). Consistent with reduced retinal thickness and diminished progenitors in $Dll4^{\Delta flox/\Delta flox}$ retinas, there was a decrease in expression of progenitor marker genes *Hes5*, *Hes6*, *Fgf15*, cyclin D1 (*Ccnd1*), and *Foxn4* in the mutant; in particular, their expression was absent from the outer edge of the mutant retina (Fig. 6 *M–V*). The expression of *Atoh7*, by contrast, appeared not to be altered in $Dll4^{\Delta flox/\Delta flox}$ retinas (Fig. 6 *W* and *X*). The reduced *Hes5* and *Ccnd1* expression is consistent with perturbed Notch signaling and diminished progenitor proliferation.

To more directly measure progenitor proliferation, we performed 5-ethynyl-2′-deoxyuridine (EdU) pulse-labeling and Ki67 immunostaining. Compared with control retinas, there were significantly fewer labeled dividing progenitor cells in E14.5 and P6 $Dll4^{\Delta flox/\Delta flox}$ retinas (Fig. S5 *A–D and K*), demonstrating an essential role for Dll4-Notch signaling in retinal progenitor proliferation. To investigate whether Dll4-Notch signaling is also required for progenitor maintenance, we measured apoptotic cell death in control and mutant retinas. There was a significant increase of TUNEL-labeled cells in E14.5 $Dll4^{\Delta flox/\Delta flox}$ retinas (Fig. S5 *E, F, and L*), suggesting that elevated cell death contributes to the decreased progenitor pool in *Dll4* mutant retinas as well. Additionally, we observed increased apoptotic cells in $Dll4^{\Delta flox/\Delta flox}$ retinas at P6 and P12, especially within the outer nuclear layer, where photoreceptor cells are located (Fig. S5 *G–J and M*). Thus, the photoreceptor cells overproduced in *Dll4* mutants may not differentiate properly and eventually degen-

erate by apoptosis over time. Interestingly, *Foxn4* inactivation also results in diminished retinal thickness, reduced retinal progenitor proliferation, and increased cell death (10).

Increased Rod Generation by *Dll4* Ablation in Postnatal Retinal Progenitors. To determine the requirement of Dll4 in late retinal progenitors, we inactivated *Dll4* in P0 retinal progenitors by transfecting via electroporation the pCAG-Cre:GFP expression plasmid (41) into P0 $Dll4^{flox/flox}$ retinas (Fig. 7*A*). Transfected retinas were collected at P12, and by immunofluorescence we used several cell type-specific markers to analyze the types of cells that were differentiated from transfected progenitors. Compared with control pCAG-GFP–transfected retinas, there was a 15.3% increase of GFP⁺ cells that coexpressed recoverin in pCAG-Cre:GFP–transfected retinas (Fig. 7 *A–D*), consistent with increased photoreceptors in $Dll4^{\Delta flox/\Delta flox}$ retinas. In agreement also with $Dll4^{\Delta flox/\Delta flox}$ mutant phenotypes, the proportions of Pax6⁺ or calbindin⁺ amacrine cells, Chx10⁺ bipolar cells, and GS⁺ Müller cells were all greatly reduced in pCAG-Cre:GFP–transfected retinas (Fig. 7 *B, E–J, M, and N*). No effect on calbindin⁺ horizontal cells or Pou4f2⁺ RGCs was observed, as these two cell types are mostly generated during embryonic stages (Fig. 7 *B* and *I–L*). Thus, Dll4-Notch signaling is required for suppressing rod fates in late retinal progenitors as well as for proper generation of other late-born cell types.

Overexpressed Dll4 Promotes Rod Formation. Apart from gene ablation, we also took a gain-of-function approach to investigate the function of Dll4 during retinal development. We overexpressed Dll4 in P0 retinal progenitors by using a replication-incompetent murine retroviral vector that carries a GFP reporter (Fig. S6*A*) (42). P0 retinas were infected by subretinal injection of Dll4-GFP and control-GFP viruses and collected at P21 for cell type analysis. Overexpressed Dll4 was expected to inhibit

Fig. 6. Altered gene expression in E14.5 $Dll4^{\Delta flox/\Delta flox}$ retinas. (*A–X*) Gene expression levels were examined by section RNA in situ hybridization analysis (*A–J* and *M–X*) or immunostaining with DAPI as counterstain (*K* and *L*). There is an increase in expression of *Otx2*, *Crx*, *Neurod1*, *Thrb*, and *Rxrg* in the outer edge of the $Dll4^{\Delta flox/\Delta flox}$ retina (*C–L*). In contrast, the expression of *Hes5*, *Hes6*, *Fgf15*, *Ccnd1*, and *Foxn4* is significantly down-regulated in the mutant retina, especially within the outer edge (marked in *N*, *P*, *R*, *T*, and *V*) (*M–V*). *Atoh7* expression does not appear to change in the mutant (*W* and *X*). inbl, inner neuroblastic layer; onbl, outer neuroblastic layer. (Scale bars: *K* and *L*, 25 μm; *A–J* and *M–X*, 50 μm.)

Notch signaling by mechanisms of lateral inhibition and *cis*-inhibition (43, 44), and therefore to enhance rod production. Indeed, overexpressed Dll4 increased the number of recoverin⁺ photoreceptors by approximately 11% (Fig. S6 *B–D*), further demonstrating the involvement of Dll4-Notch signaling in suppressing rod fates. Meanwhile, it significantly diminished Pax6⁺ or calbindin⁺ amacrine cells, Chx10⁺ bipolar cells, and GS⁺ Müller cells (Fig. S6 *B*, *E–J*, *M*, and *N*), but had no effect on early-born M-opsin⁺ cones, Pou4f2⁺ RGCs, and calbindin⁺ horizontal cells (Fig. S6 *B*, *K*, and *L*).

Discussion

Foxn4 Modulates Retinal Progenitor Fates and Proliferation by Activating *Dll4* Expression.
Our work provides genetic and biochemical data to link Foxn4 directly to Notch signaling during retinogenesis. We have shown previously that targeted disruption of *Foxn4* results in loss of most amacrine and all horizontal cells, concomitant increase of photoreceptors, and reduced progenitor proliferation (10). By a candidate gene approach, we have found that Foxn4 is required to activate *Ptf1a*, *Neurod1*, and *Neurod4* expression as the basis for its requirement for amacrine and horizontal cell generation (10). However, the underlying mechanism for its inhibition of photoreceptors and involvement in progenitor division is unclear. The identification of *Dll4* as a down-regulated gene in *Foxn4*-null retinas by microarray pro-

filing provided a clue to Notch signaling modulation as a possible mechanism.

Consistent with activation of *Dll4* expression by Foxn4, *Dll4* in situ signal was dramatically reduced in *Foxn4*-null retinas and Foxn4 colocalized with Dll4 in a subpopulation of retinal progenitors. Moreover, *Dll4* expression could be strongly induced by misexpressed Foxn4 in developing retinas. Indeed, Foxn4 appears to directly activate *Dll4* expression based on several lines of evidence: (*i*) Foxn4 can activate reporter gene expression through a 5′ and an intronic enhancer evolutionarily conserved among many vertebrate species; (*ii*) there is, in the 5′ enhancer, a cluster of four motifs of ACGC that is also present in the Foxn1 consensus DNA binding site and a zebrafish Foxn4 binding site (30, 31); (*iii*) site-directed mutagenesis of the ACGC motifs causes severe loss of reporter activity; and (*iv*) mouse and human Foxn4 can occupy the critical ACGC-containing region of the 5′ enhancer as determined by ChIP assay. Each of the four ACGC motifs in the 5′ enhancer seems to be crucial for full transcriptional activity, and they act in synergy because mutagenizing a single motif greatly reduced reporter activity whereas simultaneously mutating two or three of them completely abolished it. Despite the lack of a detailed analysis, we also found ACGC motifs in the conserved intronic enhancer CR3.

By conditionally inactivating *Dll4* in prenatal and postnatal retinal progenitors, we have demonstrated that Dll4 can indeed partly mediate the Foxn4 function in regulating progenitor fates and proliferation. Similar to *Foxn4* and *Notch1* mutant phenotypes (10, 21, 22), *Dll4* ablation leads to decreased progenitor proliferation and marker expression but increased cones and rods and up-regulated TFs involved in photoreceptor production. Thus, Foxn4 may suppress the photoreceptor competence in retinal progenitors by up-regulating Dll4-Notch signaling, which in turn represses the expression of photoreceptor TFs such as Otx2, Crx, and Thrb to inhibit the photoreceptor fates (Fig. S7*B*). It should be noted that, although photoreceptors are increased in $Foxn4^{lacZ/lacZ}$ retinas by P0 (10), our microarray data revealed up-regulated expression of several early photoreceptor marker genes, including *Otx2*, *Crx*, and *Pcdh21*, in the mutant at E14.5 (Dataset S1), suggesting that Foxn4 may be required for—rather than suppress—the differentiation of early-born photoreceptors. It will be interesting to determine how Foxn4 exerts this positive function in early photoreceptor development.

Our analysis revealed that overexpressed Dll4 in P0 retinal progenitors is able to increase photoreceptor production, presumably by inhibiting Notch signaling through mechanisms of lateral inhibition and *cis*-inhibition (43, 44). However, Dll4 overexpression in endothelial cells was found to activate Notch effectors (45). It is unclear what causes this discrepancy, but it may reflect different thresholds of activation and inhibition by Notch receptors and ligands in different cellular contexts.

Dll4 Instead of Dll1 Mediates Notch Signaling to Suppress Photoreceptor Fates.
There exist three prominent phenotypes in *Notch1* and *Rbpj* conditional mutant retinas, i.e., photoreceptor overproduction, diminished progenitor proliferation, and laminar disorganization by the formation of rosette structures (21, 22, 46, 47). It is unclear whether these phenotypes are mediated by different Notch ligands or whether each Notch ligand can similarly mediate all these phenotypes. Our analysis indicates that the *Dll4* mutant retina shares with that of the *Notch1* mutant the phenotypes of photoreceptor overproduction and diminished progenitor proliferation. This is in contrast to the *Dll1* mutant retina, in which a mild phenotype of accelerated neurogenesis is seen but photoreceptor production appears unaffected (48). Thus, Dll4 may function as the major Notch1 ligand during retinogenesis to expand the progenitor pool and limit photoreceptor generation. The third phenotype of rosette formation is severe among the *Notch1*, *Rbpj*, and *Dll1* mutants (21, 22, 46–48).
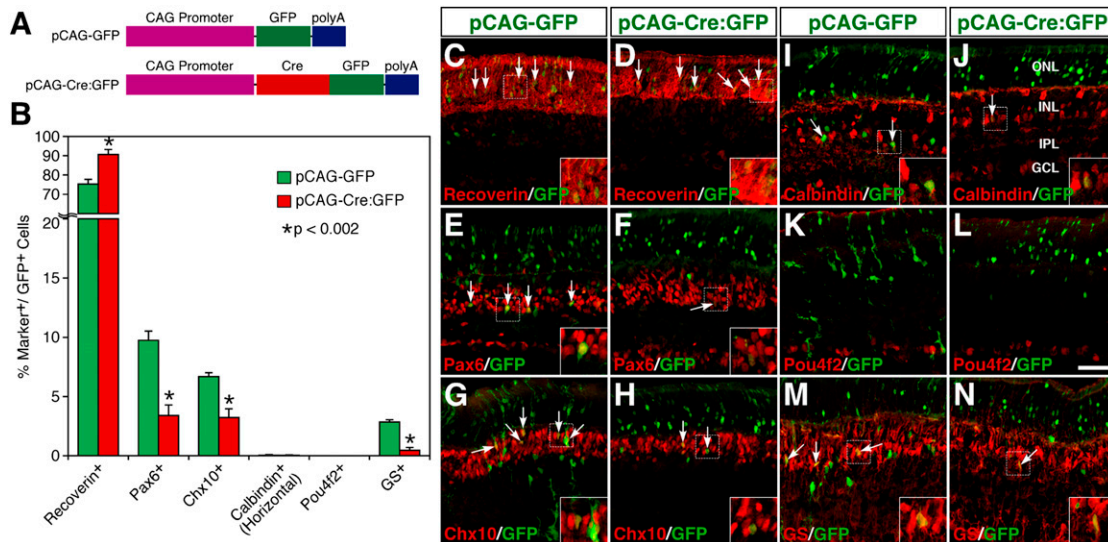
Luo et al.

Fig. 7. Inactivating *Dll4* in postnatal retinal progenitors promotes rod generation. (*A*) Schematic of pCAG-GFP and pCAG-Cre:GFP expression plasmid constructs. (*B*) Quantification of GFP⁺ cells that are immunoreactive for various cell type-specific markers. Each histogram represents the mean ± SD for three retinas. More than 500 GFP⁺ cells (ranging from 501 to 2,082 depending on frequency of colocalized cells) were scored in each retina. (*C–N*) Sections from *Dll4^flox/flox^* retinas transfected with pCAG-GFP or pCAG-Cre:GFP were double-immunostained with an anti-GFP antibody and antibodies against recoverin, Pax6, Chx10, Calbindin, Pou4f2, or GS. Cre-mediated *Dll4* ablation leads to decreased GFP⁺ in the inner nuclear layer but increased GFP⁺ cells coexpressing recoverin in the outer nuclear layer (*C* and *D*). However, it causes a significant decrease of amacrine cells immunoreactive for Pax6 or calbindin (*E*, *F*, *I*, and *J*), bipolar cells immunoreactive for Chx10 (*G* and *H*), and Müller cells immunoreactive for GS (*M* and *N*). Arrows point to representative colocalized cells and insets show corresponding outlined regions at a higher magnification. GCL, ganglion cell layer; INL, inner nuclear layer; IPL, inner plexiform layer; ONL, outer nuclear layer. (Scale bars: 43.3 μm.)

However, most regions in the *Dll4* mutant retina are free of rosettes, and they are present only in occasional regions (Figs. 4 and 5). Therefore, proper laminar organization in retinal outer layers may primarily depend on Dll1-Notch rather than Dll4-Notch signaling. It has been shown that the aberrant rosettes may be caused by defective β-catenin signaling (47).

The *Foxn4* mutant retina resembles that of the *Dll4* mutant in several aspects, including increased photoreceptors, reduced progenitor proliferation, and mild laminar disorganization. The weaker proliferation and laminar defects in *Foxn4* vs. *Dll4* mutant retinas most likely result from the fact that there is still residual *Dll4* expression in *Foxn4*-null retinas (Fig. 2). The lack of rosettes in *Foxn4*-null retinas is consistent with the near-normal expression of *Dll1* and *Notch1* in the mutant. Indeed, our misexpression analysis in retinal explants indicated that *Dll4* was the only one among several *Dll*, *Jag*, and *Notch* ligand and receptor genes that could be prominently induced by Foxn4, thereby demonstrating a rather specific regulation of Dll4-Notch signaling by Foxn4 to generate retinal cell diversity. This mechanism appears to be used by other CNS progenitors to generate neuronal diversity as well. For instance, during spinal cord development, Dll4 acts downstream of Foxn4 to specify the V2b inhibitory interneurons vs. the V2a excitatory interneurons (49, 50), whereas Dll1 is required mainly for progenitor maintenance in the V2 domain (48).

In summary, we now know that the fates of retinal progenitors during development are progressively restricted by numerous retinogenic TFs that function to establish progenitor competence, determine cell fates, and/or specify cell types and subtypes. By using a combination of bioinformatic, genetic, and biochemical approaches, we investigated the molecular basis by which Foxn4 selects the amacrine and horizontal cell fates from multipotential retinal progenitors. We provide evidence to suggest that Foxn4 has an inherent activity to inhibit the alternative photoreceptor fates of early retinal progenitors by activating the Dll4-Notch signaling (Fig. S7). Dll4 appears to partly mediate the Foxn4 function by serving as a major Notch ligand to expand the progenitor pool and limit photoreceptor production. It is therefore conceivable that, to en-

sure the highest fidelity of cell differentiation during neurogenesis, most or all competence and commitment factors may act similarly as Foxn4 to not only promote pertinent cell fates but also suppress alternative fates of multipotent progenitor/stem cells. Ultimately, it may be the balance of positive and negative influences exerted by many neurogenic factors that tips the multipotent progenitor toward a particular fate.

Materials and Methods

***Dll4* Inactivation in Postnatal Retinas.** Dll4 ablation in postnatal retinas was achieved by in vivo electroporation of a Cre expression plasmid in P0 *Dll4^flox/flox^* retinas as described previously (41). Briefly, after newborn *Dll4^flox/flox^* pups were anesthetized by chilling on ice, 0.2 μL of pCAG-Cre:GFP or pCAG-GFP (41) DNA solution (1.5 μg/μL) was injected into the subretinal space. Then square electric pulses (100 V; five 50-ms pulses with 950-ms intervals) were applied with tweezer-type electrodes (Protech). The pups were recovered in 37 °C incubator, and were fostered by CD-1 mother mice. The retinas were harvested at P12 and processed for standard immunofluorescence.

Virus Preparation and Infection. To construct the Dll4-GFP plasmid, a full-length mouse *Dll4* cDNA was ligated into the control-GFP viral vector (42). Virus preparation and infection were performed as described previously (10, 42). Retinas were infected at P0 with desired retroviruses by subretinal injection, and then harvested and analyzed at P21.

Semiquantitative RT-PCR. E17.5 CD-1 mouse retinas were dissected out in DMEM media, and then transferred into a Petri Dish Electrode (Protech). The retinas were immersed in the pCIG-Foxn4 or pCIG vector (27) DNA solutions of different concentrations (0.5 μg/μL, 1.0 μg/μL, or 2.0 μg/μL). Following square electric pulses (15 V; five 50-ms pulses with 950-ms intervals), retinal explants

www.manaraa.com

were cultured on the Millicell cell culture insert (Millipore) for 5 d. Total RNA was extracted by using TRIzol (Invitrogen) according to the manufacturer's instruction. RNA (5 μg) was used for cDNA synthesis (AMV Reverse Transcriptase; Invitrogen), and 1 μL of each cDNA was used for PCR amplification reaction. Primers used for PCR are listed in Table S1.

Dll4 Enhancer Reporter Assay. *Dll4* noncoding sequences from all available vertebrate species were retrieved using the Non-Coding Sequence Retrieval System (28). They were then aligned and compared by the online VISTA tool (http://genome.lbl.gov/vista) (29) to identify CRs. Fragments of CRs were subcloned into the reporter vector pBGP-DsRed, in which a minimal β-globin promoter was placed upstream of the DsRed gene. *Dll4* reporter plasmids were cotransfected with pCIG-Foxn4 or pCIG by electroporation into E17.5 mouse retinal explants as described earlier. Transfected retinas were cultured in vitro for 3 d. Whole-mount images were taken with a fluorescence microscope, or the retinas were fixed and processed for cryosection and staining. Mutated *Dll4* enhancer reporter plasmids were created by site-directed mutagenesis according to the manufacturer's instruction (Stratagene). ACGC motifs were muted to AAAA in all cases.

ChIP Assay. ChIP assay was performed with modification according to the protocol by Abcam (http://www.abcam.com/ps/pdf/chromatin/X-ChIP-protocol-card.pdf). Dynabeads Protein A/G (Invitrogen) was used in the experiment. Chromatin DNA was prepared from embryonic mouse retinas pooled from stages E14.5 to E17.5 or from the Y79 human retinoblastoma cells. The anti-Foxn4 antibody is commercially available (sc-66772; Santa Cruz). The PCR primers used are as follows: for mouse retina, 5′GGCTAGAGAAGTTGATTTCC (a) and 5′GGCTAGAGAAGTTGATTTTCC (b); or 5′GATTTATTGACCGGCAGGTGCG (c) and 5′GAGGCCGGCGCGTGCCTCATC (d). Primers 5′AAGAGTCGCACCGGCTCTGCAC and 5′CAAGCCTCCTCTCTGCTTTCTC were used to amplify the Dll4 3′ UTR. For Y79 cells, primers are 5′GATTTATTGACCGGCAGGTGCG and 5′TGG-CTGCTCCATTCGATCCATTC.

Immunostaining. All immunofluorescence staining was performed on cryosections. Tissue processing and staining procedures were described previously (10, 42). The following primary antibodies were used: mouse anti-Pou4f1 (Millipore); rabbit and goat anti-Pou4f2 (Santa Cruz); rabbit and mouse anti–calbindin D-28k (Swant); rabbit anti-Foxn4 (10); sheep anti-Chx10 (Exalpha); rabbit, chicken, and goat anti-GFP (MBL International, Abcam, and Biogenesis, respectively); mouse anti-Ki67 (BD Pharmingen); mouse anti-GAD67 (Millipore); rabbit anti-Sox9 (Millipore); mouse anti-glutamine synthetase (Millipore); rabbit anti-RXRγ/Rxrg (Santa Cruz); goat anti-GLYT1 (Millipore); rabbit and mouse anti-Pax6 (Millipore and DSHB, respectively); goat anti-Dll4 (R&D Systems); rabbit anti-recoverin (Millipore); and mouse anti-rhodopsin (Sigma). DAPI, YOPRO1, and TOPRO3 (Invitrogen) were used for nuclear counterstaining. Images were captured with a Nikon Eclipse 80i microscope or a laser scanning Leica TCS-SP2 confocal microscope. Quantification of immunoreactive cells was carried out as previously described (51).

Microarray Profiling, In Situ Hybridization, Edu Labeling, and TUNEL Labeling. Microarray profiling and analysis were performed as previously described (18) by using probes derived from retinal RNA of E14.5 *Foxn4*$^{+/+}$ and *Foxn4*$^{lacZ/lacZ}$ embryos (10).

RNA in situ hybridization was carried out as described previously (42, 52). Digoxigenin-labeled riboprobes were prepared following the manufacturer's protocol (Roche Diagnostics). The probes for *Foxn4*, *Atoh7*, *Neurod1*, *Crx*, *Otx2*, *Thrb*, *Hes1*, *Hes5*, and *Notch1* were described previously (10, 18). *Dll1*, *Dll4*, *Rbpj*, *Hey1*, *Hes6*, *Fgf15*, and *Ccnd1* probes were amplified by PCR from mouse retinal cDNA, and cloned into the PCR II (Invitrogen) or PSC-A (Stratagene) vectors.

For Edu labeling, the Click-iT EdU labeling kit was purchased from Invitrogen. Timed pregnant mice were injected with EdU solution (30 μg/g body weight) and killed 1.5 h later. Embryos were collected, fixed, and processed according to standard immunostaining protocol. EdU staining was performed according to the procedure provided by the kit.

TUNEL assay was performed as previously described using the In Situ Cell Death Detection Kit TMR Red (Roche Diagnostics) (10).

1. Sidman RL (1961) Histogenesis of mouse retina studied with thymidine-^{3}H. *The Structure of the Eye*, ed Smelser G (Academic, New York), pp 487–506.
2. Young RW (1985) Cell differentiation in the retina of the mouse. *Anat Rec* 212:199–205.
3. Cepko CL (1999) The roles of intrinsic and extrinsic cues and bHLH genes in the determination of retinal cell fates. *Curr Opin Neurobiol* 9:37–46.
4. Livesey FJ, Cepko CL (2001) Vertebrate neural cell-fate determination: Lessons from the retina. *Nat Rev Neurosci* 2:109–118.
5. Harris WA (1997) Cellular diversification in the vertebrate retina. *Curr Opin Genet Dev* 7:651–658.
6. Marquardt T, et al. (2001) Pax6 is required for the multipotent state of retinal progenitor cells. *Cell* 105:43–55.
7. Taranova OV, et al. (2006) SOX2 is a dose-dependent regulator of retinal neural progenitor competence. *Genes Dev* 20:1187–1202.
8. Matsushima D, Heavner W, Pevny LH (2011) Combinatorial regulation of optic cup progenitor cell fate by SOX2 and PAX6. *Development* 138:443–454.
9. Elliott J, Jolicoeur C, Ramamurthy V, Cayouette M (2008) Ikaros confers early temporal competence to mouse retinal progenitor cells. *Neuron* 60:26–39.
10. Li S, et al. (2004) Foxn4 controls the genesis of amacrine and horizontal cells by retinal progenitors. *Neuron* 43:795–807.
11. Fujitani Y, et al. (2006) Ptf1a determines horizontal and amacrine cell fates during mouse retinal development. *Development* 133:4439–4450.
12. Nakhai H, et al. (2007) Ptf1a is essential for the differentiation of GABAergic and glycinergic amacrine cells and horizontal cells in the mouse retina. *Development* 134:1151–1160.
13. Inoue T, et al. (2002) Math3 and NeuroD regulate amacrine cell fate specification in the retina. *Development* 129:831–842.
14. Nishida A, et al. (2003) Otx2 homeobox gene controls retinal photoreceptor cell fate and pineal gland development. *Nat Neurosci* 6:1255–1263.
15. Chen J, Rattner A, Nathans J (2005) The rod photoreceptor-specific nuclear receptor Nr2e3 represses transcription of multiple cone-specific genes. *J Neurosci* 25:118–129.
16. Corbo JC, Cepko CL (2005) A hybrid photoreceptor expressing both rod and cone genes in a mouse model of enhanced S-cone syndrome. *PLoS Genet* 1:e11.
17. Peng GH, Ahmad O, Ahmad F, Liu J, Chen S (2005) The photoreceptor-specific nuclear receptor Nr2e3 interacts with Crx and exerts opposing effects on the transcription of rod versus cone genes. *Hum Mol Genet* 14:747–764.
18. Qiu F, Jiang H, Xiang M (2008) A comprehensive negative regulatory program controlled by Brn3b to ensure ganglion cell specification from multipotential retinal precursors. *J Neurosci* 28:3392–3403.
19. Wang SW, et al. (2001) Requirement for *math5* in the development of retinal ganglion cells. *Genes Dev* 15:24–29.
20. Brown NL, Patel S, Brzezinski J, Glaser T (2001) Math5 is required for retinal ganglion cell and optic nerve formation. *Development* 128:2497–2508.
21. Jadhav AP, Mason HA, Cepko CL (2006) Notch 1 inhibits photoreceptor production in the developing mammalian retina. *Development* 133:913–923.
22. Yaron O, Farhy C, Marquardt T, Applebury M, Ashery-Padan R (2006) Notch1 functions to suppress cone-photoreceptor fate specification in the developing mouse retina. *Development* 133:1367–1378.
23. Li C, Wong WH (2003) DNA-Chip Analyzer (dChip). *The Analysis of Gene Expression Data: Methods and Software*, eds Parmigiani G, Garrett ES, Irizarry R, Zeger SL (Springer-Verlag, New York), pp 120–141.
24. Dennis G, Jr., et al. (2003) DAVID: Database for Annotation, Visualization, and Integrated Discovery. *Genome Biol* 4:3.
25. Dyer MA, Livesey FJ, Cepko CL, Oliver G (2003) Prox1 function controls progenitor cell proliferation and horizontal cell genesis in the mammalian retina. *Nat Genet* 34:53–58.
26. Morrow EM, Furukawa T, Lee JE, Cepko CL (1999) NeuroD regulates multiple functions in the developing neural retina in rodent. *Development* 126:23–36.
27. Jin K, Jiang H, Mo Z, Xiang M (2010) Early B-cell factors are required for specifying multiple retinal cell types and subtypes from postmitotic precursors. *J Neurosci* 30:11902–11916.
28. Doh ST, Zhang Y, Temple MH, Cai L (2007) Non-coding sequence retrieval system for comparative genomic analysis of gene regulatory elements. *BMC Bioinformatics* 8:94.
29. Frazer KA, Pachter L, Poliakov A, Rubin EM, Dubchak I (2004) VISTA: Computational tools for comparative genomics. *Nucleic Acids Res* 32(web server issue):W273-9.
30. Schlake T, Schorpp M, Nehls M, Boehm T (1997) The nude gene encodes a sequence-specific DNA binding protein with homologs in organisms that lack an anticipatory immune system. *Proc Natl Acad Sci USA* 94:3842–3847.
31. Chi NC, et al. (2008) Foxn4 directly regulates *tbx2b* expression and atrioventricular canal formation. *Genes Dev* 22:734–739.
32. Poulaki V, et al. (2009) Molecular sequelae of histone deacetylase inhibition in human retinoblastoma cell lines: Clinical implications. *Invest Ophthalmol Vis Sci* 50:4072–4079.
33. Hozumi K, et al. (2008) Delta-like 4 is indispensable in thymic environment specific for T cell development. *J Exp Med* 205:2507–2513.
34. Li S, Misra K, Xiang M (2010) A Cre transgenic line for studying V2 neuronal lineages and functions in the spinal cord. *Genesis* 48:667–672.
35. Furuta Y, Lagutin O, Hogan BL, Oliver GC (2000) Retina- and ventral forebrain-specific Cre recombinase activity in transgenic mice. *Genesis* 26:130–132.
36. Furukawa T, Morrow EM, Li T, Davis FC, Cepko CL (1999) Retinopathy and attenuated circadian entrainment in *Crx*-deficient mice. *Nat Genet* 23:466–470.
37. Liu H, et al. (2008) NeuroD1 regulates expression of thyroid hormone receptor 2 and cone opsins in the developing mouse retina. *J Neurosci* 28:749–756.

Luo et al.

38. Pennesi ME, et al. (2003) *BETA2/NeuroD1* null mice: A new model for transcription factor-dependent photoreceptor degeneration. *J Neurosci* 23:453–461.

39. Ng L, et al. (2001) A thyroid hormone receptor that is required for the development of green cone photoreceptors. *Nat Genet* 27:94–98.

40. Roberts MR, Hendrickson A, McGuire CR, Reh TA (2005) Retinoid X receptor (γ) is necessary to establish the S-opsin gradient in cone photoreceptors of the developing mouse retina. *Invest Ophthalmol Vis Sci* 46:2897–2904.

41. Matsuda T, Cepko CL (2007) Controlled expression of transgenes introduced by in vivo electroporation. *Proc Natl Acad Sci USA* 104:1027–1032.

42. Mo Z, Li S, Yang X, Xiang M (2004) Role of the *Barhl2* homeobox gene in the specification of glycinergic amacrine cells. *Development* 131:1607–1618.

43. del Álamo D, Rouault H, Schweisguth F (2011) Mechanism and significance of cis-inhibition in Notch signalling. *Curr Biol* 21:R40–R47.

44. Sprinzak D, et al. (2010) Cis-interactions between Notch and Delta generate mutually exclusive signalling states. *Nature* 465:86–90.

45. Trindade A, et al. (2008) Overexpression of delta-like 4 induces arterialization and attenuates vessel formation in developing mouse embryos. *Blood* 112:1720–1729.

46. Riesenberg AN, Liu Z, Kopan R, Brown NL (2009) Rbpj cell autonomous regulation of retinal ganglion cell and cone photoreceptor fates in the mouse retina. *J Neurosci* 29:12865–12877.

47. Zheng MH, et al. (2009) The transcription factor RBP-J is essential for retinal cell differentiation and lamination. *Mol Brain* 2:38.

48. Rocha SF, Lopes SS, Gossler A, Henrique D (2009) Dll1 and Dll4 function sequentially in the retina and pV2 domain of the spinal cord to regulate neurogenesis and create cell diversity. *Dev Biol* 328:54–65.

49. Peng CY, et al. (2007) Notch and MAML signaling drives Scl-dependent interneuron diversity in the spinal cord. *Neuron* 53:813–827.

50. Del Barrio MG, et al. (2007) A regulatory network involving Foxn4, Mash1 and delta-like 4/Notch1 generates V2a and V2b spinal interneurons from a common progenitor pool. *Development* 134:3427–3436.

51. Jiang H, Xiang M (2009) Subtype specification of GABAergic amacrine cells by the orphan nuclear receptor Nr4a2/Nurr1. *J Neurosci* 29:10449–10459.

52. Liu W, Mo Z, Xiang M (2001) The *Ath5* proneural genes function upstream of Brn3 POU domain transcription factor genes to promote retinal ganglion cell development. *Proc Natl Acad Sci USA* 98:1649–1654.

www.manaraa.com